Spin excitations and mechanisms of superconductivity in cuprates

N. M. Plakida [1)]

Joint institute for Nuclear Research, Dubna, Moscow reg. 141980, Russia

A microscopic theory of spin excitations in strongly-correlated electronic systems within the 2D t–J model is discussed. An exact representation for the the dynamic spin susceptibility is derived. In the normal state, the excitation spectrum reveals a crossover from spin-wave-like excitations at low doping to overdamped paramagnon excitations above the optimal doping. In the superconducting state, the resonance mode (RM) at the antiferromagnetic wave vector $\mathbf{Q} = \pi(1,1)$ appears which is explained by a strong suppression of the spin excitation damping at low temperatures caused by a spin gap at $\mathbf{Q}$ rather than by opening of a superconducting gap. The energy of the RM is temperature independent and is observed even above T_c in the underdoped region in agreement with experiments on YBCO compounds. A major role of spin excitations in superconducting pairing in cuprates is stressed in discussing mechanisms of high-T_c superconductivity.

Recent studies of charge- spin-excitation spectra using angle-resolved photoemission (ARPES) and inelastic neutron scattering (INS) have revealed an important role of antiferromagnetic (AF) spin excitations in the "kink" phenomenon and the d-wave pairing in cuprates. In particular, in Ref. [1] a quantitative analysis of the AF spin-excitation spectrum measured by INS and of ARPES data for the spin-fermion coupling on the same $YBa_2Cu_3O_{6.6}$ ($YBCO_{6.6}$) crystal has enabled to solve the Eliashberg equation and to estimate the superconducting transition temperature which exceeds $T_c = 150$ K.

The main argument against the spin-fluctuation pairing, the weak intensity of spin fluctuations at the optimal doping seen in the INS experiments [2], was dismissed in recent resonant inelastic x-ray scattering (RICS) [3]. In a large family of cuprate superconductors paramagnon AF excitations with dispersions and spectral weights similar to those of magnons in undoped cuprates were found. A numerical solution of the Eliashberg equations for the magnetic spectrum found in $YBCO_7$ results in $T_c = 100 - 200$ K.

In this report we present a microscopic theory of spin-excitation spectrum in strongly correlated electronic systems (SCES) [4, 5] to be used in further investigation of the spin-fluctuation pairing mechanism.

1. Dynamic spin susceptibility. To describe the low-energy spin excitations in SCES the one-subband t–J model can be used:

$$H = \sum_{i\neq j,\sigma} t_{ij}\, \hat{c}^{\dagger}_{i\sigma}\hat{c}_{j\sigma} + \frac{1}{2}\sum_{i\neq j} J_{ij}\, (\mathbf{S}_i\mathbf{S}_j - \frac{n_i n_j}{4}), \quad (1)$$

where t_{ij} is the hopping integral and J_{ij} is the exchange interaction. Here $\hat{c}^{\dagger}_{i\sigma} = c^{\dagger}_{i\sigma}\,(1 - n_{i,-\sigma})$ are the projected fermion operators acting in the the singly occupied subband and $n_i = \sum_{\sigma} n_{i,\sigma}$, $n_{i,\sigma} = \hat{c}^{\dagger}_{i\sigma}\hat{c}_{i\sigma}$. $S^{\alpha}_i = (1/2)\sum_{\sigma\sigma'} \hat{c}^{\dagger}_{i\sigma}\tau^{\alpha}_{\sigma\sigma'}\hat{c}_{i\sigma'}$ are the spin-1/2 operators where $\tau^{\alpha}_{\sigma\sigma'}$ are the Pauli matrices, $\sigma = \pm 1$.

Using the Mori projection technique [6], an exact representation for the dynamical spun susceptibility (DSS) determined by the retarded Green function (GF) of the transverse spin-density operators $S^{\pm}_{\mathbf{q}} = S^{x}_{\mathbf{q}} \pm iS^{y}_{\mathbf{q}}$ can be derived [7] (see also [8]):

$$\chi(\mathbf{q},\omega) = -\langle\langle S^{+}_{\mathbf{q}} | S^{-}_{-\mathbf{q}}\rangle\rangle_{\omega} = \frac{m(\mathbf{q})}{\omega^2_{\mathbf{q}} + \omega\,\Sigma(\mathbf{q},\omega) - \omega^2}, \quad (2)$$

where $m(\mathbf{q}) = \langle [i\dot{S}^{+}_{\mathbf{q}}, S^{-}_{-\mathbf{q}}]\rangle = \langle [\,[S^{+}_{\mathbf{q}}, H],\, S^{-}_{-\mathbf{q}}]\rangle$, and $\omega_{\mathbf{q}}$ is the spin-excitation spectrum in the generalized mean-field approximation (GMFA). The self-energy is given by the Kubo-Mori relaxation function

$$\Sigma(\mathbf{q},\omega) = [1/m(\mathbf{q})]\,((-\ddot{S}^{+}_{\mathbf{q}} \,|\, -\ddot{S}^{-}_{-\mathbf{q}}))^{(\mathrm{pp})}_{\omega}\,, \quad (3)$$

where $-\ddot{S}^{\pm}_{\mathbf{q}} = [\,[S^{\pm}_{\mathbf{q}}, H],\, H]$. The relaxation function is related to the GF by the equation: $\omega((A|B))_{\omega} = \langle\langle A|B\rangle\rangle_{\omega} - \langle\langle A|B\rangle\rangle_{\omega=0}$. The "proper part" (pp) of the relaxation function (3) describes the projected time evolution as in the original Mori projection technique. The static susceptibility in (2) is defined by the equation $\chi_{\mathbf{q}} = \chi(\mathbf{q},0) = m(\mathbf{q})/\omega^2_{\mathbf{q}}$. The spin-excitation spectrum $\omega_{\mathbf{q}}$ was calculated from the equality $m(\mathbf{q}) = (-\ddot{S}^{+}_{\mathbf{q}}, S^{-}_{-\mathbf{q}}) = \omega^2_{\mathbf{q}}\,(S^{+}_{\mathbf{q}}, S^{-}_{-\mathbf{q}})$, where the correlation function $(-\ddot{S}^{+}_{\mathbf{q}}, S^{-}_{-\mathbf{q}})$ was evaluated in the GMFA [4].

The self-energy (3) is defined in terms of the force operators $-\ddot{S}^{\pm}_i = [[S^{\pm}_i, (H_t + H_J)], (H_t + H_J)] \equiv \sum_{\alpha} F^{\alpha}_i$ ($\alpha = tt, tJ, Jt, JJ$), where H_t and H_J are the hopping and the exchange parts of the Hamiltonian (1). There are 16 contributions of the type $((F^{\alpha}_{\mathbf{q}}\,|F^{\gamma}_{-\mathbf{q}}))_{\omega}$. At a finite hole doping $\delta > 0.05$ the largest contribution to the self-energy (3) is given by

[1)]plakida@theor.jinr.ru

the term $\Sigma_t(\mathbf{q},\omega) = \langle\langle F^{tt}_{\mathbf{q}} | F^{tt}_{-\mathbf{q}} \rangle\rangle_\omega / m(\mathbf{q})$ caused by spin-electron scattering [4],

$$F^{tt}_i = \sum_{j,n} t_{ij} \Big\{ t_{jn} \left[H^{-}_{ijn} + H^{+}_{nji} \right] - (i \Longleftrightarrow j) \Big\}, \quad (4)$$

where $H^{-}_{ijn} = \hat{c}^{\dagger}_{i\sigma} S^{-}_{j} \hat{c}_{n\sigma} + \hat{c}^{\dagger}_{i\downarrow}(1 - n_{j,-\sigma})\hat{c}_{n\uparrow}$. We calculate the self-energy in the the mode-coupling approximation assuming independent propagation of electronic ($\hat{c}^{\dagger}_{i\sigma}$) and bosonic ($S^{+}_{j}, n_{i,\sigma}$) excitations at different lattice sites, $i \neq j, j \neq n$, in (4):

$$\langle \hat{c}^{\dagger}_{i\sigma} S^{-}_{j} \hat{c}_{n\sigma} | \hat{c}^{\dagger}_{n'\sigma}(t) S^{+}_{j'}(t) \hat{c}_{i'\sigma}(t) \rangle = \langle \hat{c}^{\dagger}_{i\sigma} \hat{c}_{i'\sigma}(t) \rangle \, \langle S^{-}_{j} S^{+}_{j'}(t) \rangle \, \langle \hat{c}_{n\sigma} \hat{c}^{\dagger}_{n'\sigma}(t) \rangle \, . \quad (5)$$

In the superconducting state anomalous correlation functions $\langle \hat{c}^{\dagger}_{i,-\sigma} \hat{c}^{\dagger}_{n'\sigma}(t) \rangle \langle S^{-}_{j} S^{+}_{j'}(t) \rangle \, \langle \hat{c}_{n\sigma} \hat{c}_{i',-\sigma}(t) \rangle$ have to be also taken into account. Using the spectral representation for the correlation functions in (5) the imaginary part of the self-energy can be written as [5]:

$$\Sigma''_t(\mathbf{q},\omega) = -\frac{\pi (2t)^4 (e^{\beta\omega} - 1)}{m(\mathbf{q})\,\omega} \int\!\!\int\!\!\int_{-\infty}^{\infty} d\omega_1 d\omega_2 d\omega_3$$
$$\frac{1}{N^2} \sum_{\mathbf{q_1},\mathbf{q_2}} N(\omega_2)[1 - n(\omega_1)] n(\omega_3) \delta(\omega + \omega_1 - \omega_2 - \omega_3)$$
$$B_{\mathbf{q_2}}(\omega_2) \big[(\Lambda^2_{\mathbf{q_1},\mathbf{q_2},\mathbf{q_3}} + \Lambda^2_{\mathbf{q_3},\mathbf{q_2},\mathbf{q_1}}) \, A^{N}_{\mathbf{q_1}}(\omega_1) \, A^{N}_{\mathbf{q_3}}(\omega_3)$$
$$-2\Lambda_{\mathbf{q_1},\mathbf{q_2},\mathbf{q_3}} \Lambda_{\mathbf{q_3},\mathbf{q_2},\mathbf{q_1}} \, A^{S}_{\mathbf{q_1}\sigma}(\omega_1) \, A^{S}_{\mathbf{q_3}\sigma}(\omega_3) \big] . \quad (6)$$

The interaction is defined by the nearest-neighbor hopping integral t and $\Lambda_{\mathbf{q_1}\mathbf{q_2}\mathbf{q_3}} = 4(\gamma_{\mathbf{q_3}+\mathbf{q_2}} - \gamma_{\mathbf{q_1}})\,\gamma_{q_3} + \gamma_{\mathbf{q_2}} - \gamma_{\mathbf{q_1}+\mathbf{q_3}}$, $\mathbf{q_3} = \mathbf{q} - \mathbf{q_1} - \mathbf{q_2}$, $\gamma_{\mathbf{q}} = 1/2(\cos q_x + \cos q_y)$. Here $A^{N}_{\mathbf{q}}(\omega) = -(1/\pi)\mathrm{Im}\langle\langle \hat{c}_{\mathbf{q}\sigma} | \hat{c}^{\dagger}_{\mathbf{q}\sigma} \rangle\rangle_\omega$ and $A^{S}_{\mathbf{q}\sigma}(\omega) = -(1/\pi)\mathrm{Im}\langle\langle \hat{c}_{\mathbf{q}\sigma} | \hat{c}_{-\mathbf{q},-\sigma} \rangle\rangle_\omega$, are the electronic and $B_{\mathbf{q}}(\omega) = (1/\pi)\,\chi''(\mathbf{q},\omega)$ is the spin-excitation spectral functions. $n(\omega) = (e^{\beta\omega} + 1)^{-1}$ and $N(\omega) = (e^{\beta\omega} - 1)^{-1}$ are the Fermi and Bose functions.

2. Spin dynamics in the normal state. The spectrum of spin excitations $\omega_{\mathbf{q}}$ and the damping $\Gamma_{\mathbf{q}} = -(1/2)\Sigma''(\mathbf{q},\omega_{\mathbf{q}})$ were calculated using the imaginary part of the self-energy in the normal state $\Sigma''_t(\mathbf{q},\omega)$ (6) and a similar expression for the self-energy $\Sigma''_J(\mathbf{q},\omega)$ caused by the exchange interaction, $F^{J}_i = [[S^{+}_i, H_J)], H_J]$. The electronic spectral function $A^{S}_{\mathbf{q}\sigma}(\omega)$ was calculated in the Hubbard I approximation while for $B_{\mathbf{q}}(\omega)$ the GMFA was used. In the Heisenberg limit at $\delta = 0$ the spectrum of spin excitations and the damping $\Gamma_{J,\mathbf{q}}$ are shown in Fig. 1. Well-defined quasiparticle excitations with $\Gamma_{\mathbf{q}} \ll \omega_{\mathbf{q}}$ characteristic to the Heisenberg model are found. However, for non-zero doping the spin-electron scattering contribution $\Sigma''_t(\mathbf{q},\omega)$ (6) increases rapidly with doping and temperature and already at moderate hole concentration far exceeds the spin-spin scattering contribution $\Sigma''_J(\mathbf{q},\omega)$ as demonstrated in Fig. 2. We

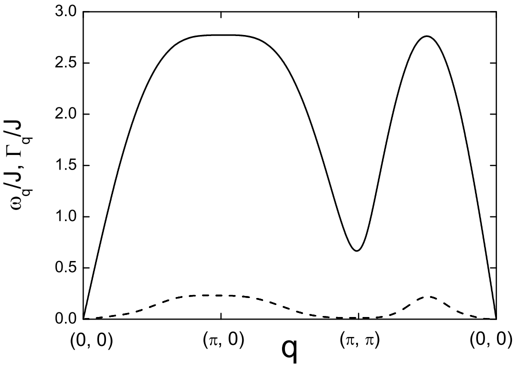

Fig. 1. Spectrum $\omega_{\mathbf{q}}$ (solid line) and damping $\Gamma_{J,\mathbf{q}}$ (dashed line) in the Heisenberg limit, $\delta = 0$, at $T = 0.35J$.

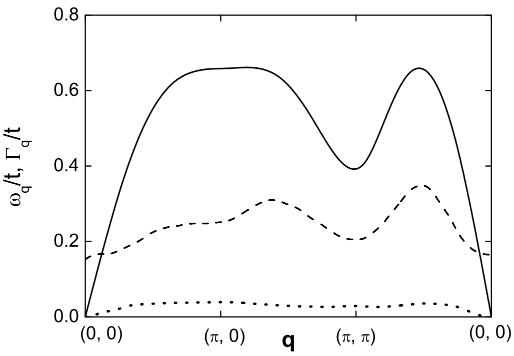

Fig. 2. Spectrum $\omega_{\mathbf{q}}$ (solid line), damping $\Gamma_{J,\mathbf{q}}$ (dotted line) and $\Gamma_{t,\mathbf{q}}$ (dashed line) at $T = 0.15t$ and $\delta = 0.1$.

conclude, that at low enough doping and low temperatures well-defined spin-wave-like excitations propagating in the AF short-range order background are observed, while for higher doping and temperatures a crossover to AF paramsgnon-like spin excitations occurs as found in INS experiments [2, 9].

3. Magnetic resonance mode. In the superconducting state the spin-excitation spectrum of high-T_{c} cuprates is dominated by a sharp magnetic peak at the AF wave vector $\mathbf{Q}$ which is called *the resonance mode* (RM) [2]. The RM energy E_{r} decreases with underdoping scaling with T_{c}: $E_{\mathrm{r}} \simeq 5.3 k_{\mathrm{B}} T_{\mathrm{c}}$, but only weakly depends on temperature (see, e.g. [10, 11]).

The RM was often studied within the spin-fermion models using the random phase approximation (RPA) for the DSS. In this approach, the opening of the energy gap $2\Delta_{\mathbf{q}}$ in the particle-hole continuum of excitations below T_{c} results in the appearance of the RM as a bound state (spin-exciton) at the energy $E_{\mathrm{r}} < 2\Delta_{\mathbf{q}}$. However, in this scenario a strong temperature dependence of the RM driven by $2\Delta(T)$ should be observed which has not been found in experiments.

In our theory the self-energy (6) is determined by the decay of a spin excitation with the energy ω and

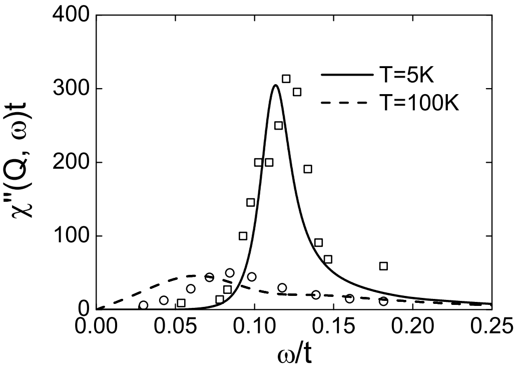

Fig. 3. Spectral function for doping $\delta = 0.2$ compared to experimental data [2], at $T = 5K$ (squares) and $T = 100K$ (circles).

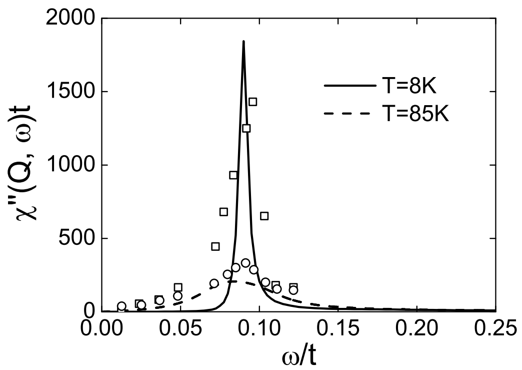

Fig. 4. Spectral function for doping $\delta = 0.09$ compared to experimental data [10] at $T = 8K$ (squares) and $T = 85K$ (circles).

the wave vector $\mathbf{q}$ into three excitations: a particle-hole pair and a spin excitation. This process is controlled by the energy and momentum conservation laws, $\omega = (\omega_3 - \omega_1) + \omega_2$ and $\mathbf{q} = \mathbf{q}_1 + \mathbf{q}_2 + \mathbf{q}_3$, which is quite different from the RPA calculations where in the decay process only the particle-hole pair is taken into account. In several studies of the self-energy in the t-J model the contribution of the additional spin excitation was neglected or approximated by static or mean-field-type expressions (see, e.g., [8]). This approximation results in the RPA-type DSS and in a similar temperature dependence of the RM.

We have calculated the spectral function $\chi''(\mathbf{Q}, \omega)$ using the self-energy (6) and assuming the d-wave gap function $\Delta_{\mathbf{q}} = (\Delta/2)(\cos q_x - \cos q_y)$ in the superconducting state. The DSS reveals a pronounced RM at low temperatures and a weak temperature dependence at $T \lesssim T_c$ due to a strong suppression of damping of spin excitations. This is explained by an involvement of a spin excitation in the decay process as explained above. Due to the spin gap in the spin-excitation spectrum at $\mathbf{Q}$ (see Figs. 1, 2) the spin excitation with the energy $\omega_2 \simeq \omega_{\mathbf{Q}}$ in this process plays a dominant role in limiting the decay of the RM in comparison with the superconducting gap in the particle-hole excitation. Since $\omega_{\mathbf{Q}}$ shows a weak temperature dependence at $T \lesssim T_c$ the RM does not reveal an appreciable temperature dependence and can be observed even above T_c in the underdoped region.

Figure 3 shows the temperature dependence of the spectral functions in the overdoped case at $\delta = 0.2$ and experimental data (symbols) for $YBCO_{6.92}$ [2]. The RM having a high intensity at low temperatures strongly decreases with temperature and becomes very broad at $T \sim T_c$. The spectral function for the underdoped case $\delta = 0.09$ is plotted Fig. 3. The RM shows a weak temperature dependence and is still visible even at $T = 85$ K$= 1.4\,T_c$ as found in the INS experiment on $YBCO_{6.5}$ [10] shown by symbols.

Thus, as compared with the spin-exciton scenario based on the bubble-type approximation, we propose an alternative explanation of the RM which is driven by the spin gap at $\mathbf{Q}$ rather than by opening of the superconducting gap.

4. Remarks on mechanisms of superconductivity in cuprates. Despite of intensive search for the mechanism of high-temperature superconductivity in cuprates, there is still no commonly accepted theory (for a review see [12]). Below we briefly discuss two most widely studied mechanisms of superconductivity in cuprates caused by spin fluctuations and by electron-phonon interaction.

At first we consider the microscopic theory of pairing induced by kinematic interaction within the t–J [13] and the Hubbard [14] models. In the models, strong electron correlations are rigorously taken into account by applying the Hubbard operator technique. It was shown that there are two channels of pairing. The first one is mediated by inter-subband hopping determined by the non-retarded AF exchange interaction $J(\mathbf{k} - \mathbf{k}')$. The AF pairing occurs for all electrons in the conducting subband of the width $W \sim 2$ eV that results in $T_c^{ex} \simeq [\mu(W - \mu)]^{1/2} \exp(-1/V_{ex})$ proportional to the Fermi energy $\mu \sim 0.5$ eV measured from the bottom of the band. Therefore, T_c^{ex} can be large even for a weak coupling $V_{ex} = J\,N(0) \sim 0.2$. The second spin-fluctuation (sf) pairing channel is induced by the intra-subband hopping. The sf-pairing is restricted to a range of energies $\omega_s \sim J$ near the FS, as in the BCS theory, with $T_c^{sf} \simeq \omega_s \exp(-1/V_{sf})$, $V_{sf} = \lambda_{sf}\,N(0)$. The effective spin-fluctuation coupling constant is given by the hopping parameter $t(\mathbf{k})$ averaged over the Fermi surface: $\lambda_{sf} \simeq \langle t^2(\mathbf{k}) \rangle_{\rm FS}/\omega_s \sim t^2/J \sim 1$ eV. The interaction appears to be quite large and is comparable with the value found in ARPES [1]. Taking into account both contributions, an estimate for

T_c can be written as $T_c = \omega_s \exp(-1/\widetilde{V}_{sf})$ where $\widetilde{V}_{sf} = V_{sf} + V_{ex}/[1 - V_{ex}\ln(\mu/\omega_s)]$. Here the coupling constant $\widetilde{V}_{sf}$ is strongly enhanced by the second term that results in high-temperature superconductivity.

The electron-phonon (e-ph) pairing mechanism advocated in a number of publications (see the reviews [15, 16]) demands a strong e-ph coupling interaction, $1 < \lambda_{ep} < 3.5$, for phonon modes of a particular symmetry to provide the d-wave pairing. However, the "first-principle" (LDA) calculations show rather small coupling $\lambda_{ep} < 0.3$ for these modes (see, e.g., [17]). It would be difficult to prove that allowing for strong electron correlations in LDA an order of magnitude increase of λ_{ep} could be achieved.

Strong electron-phonon interaction observed in polaronic effects may be irrelevant for the d-wave pairing. In particular, polaronic effects found in the magnetic penetration depth (see, e.g., [18]) give no contribution to the d-wave pairing contrary to claim in Ref. [19]. To demonstrate this, let us consider the oxygen-isotope effect (OIE) on T_c by taking into account polaronic effect on the magnetic penetration depth. The latter is ascribed to the effective polaron mass renormalization, $m^*/m = \exp(\gamma E_p/\omega) = \exp 2\beta$ (see, [20]). The exponent β weakly depends on hole concentrations, e.g., $\beta = 1 - 0.6$ for $x = 0.06 - 0.15$ in $La_{2-x}Sr_xCuO_4$ [19]. For a qualitative discussion, we consider the conventional BCS formula for $T_c \approx \omega \exp(-1/\lambda)$ where the polaronic band narrowing effect results in increase of the coupling constant, $\lambda = \lambda_0(m^*/m)$. Then for the isotope exponent on T_c we obtain $\alpha = -(d \ln T_c/d \ln M) = 1/2 - \beta/\lambda$. From this expression follows that contrary to experiments, for underdoped compounds with large β and small λ (low T_c) the isotope exponent α would be smaller than for optimally doped compounds with lower values of β and larger coupling λ. In particular, for $\lambda \leq 1$ the isotope exponent $\alpha \sim -0.5$ that contradicts to all experiments [18]. (For the McMillan formula for T_c we obtain even larger reduction of α). Thus, the large polaronic effect in the effective mass cannot explain doping dependence of the OIE on T_c and therefore is irrelevant to the superconducting d-wave pairing in cuprates.

A large e-ph coupling constant inferred from tunneling experiments [16] where the spectral function $\alpha^2F(\omega)$ averaged over the Fermi surface was extracted in terms of s-wave pairing may be unreliable. A generalization of the McMillan-Rowell procedure to d-wave superconductors should be used for extracting the spectral function $\alpha^2(\mathbf{k},\mathbf{k}')F(\mathbf{k},\mathbf{k}',\omega)$ from tunneling experiments. A proper consideration of the atomic-scale disorder should be also taken into account [21].

The spectral function in the normal sate deduced from high-resolution laser ARPES [22] revealed the intrinsic upper cutoff energy of about 400 meV, far beyond phonon energies. Similar high-resolution ARPES studies of the anomalous self-energy (the gap function) are required to find out the pairing "$l = 2$" component of the spectral function responsible for d-wave superconductivity (see [23]).

In summary, whereas the microscopic theory within the Hubbard and the t–J models can provide the AF exchange and spin-fluctuation pairing mechanism in cuprates which is supported by recent INS and RICS experiments, the e-ph pairing mechanism still needs to be proved. It is most likely that both contributions, with a proper account of strong electron correlations, are important for developing a consistent theory of superconductivity in cuprates.

References

1. T. Dahm, et al., Nature Physics **5**, 780 (2009).
2. Ph. Bourges, in: *The Gap Symmetry and Fluctuations in High Temperature Superconductors*, ed. by J. Bok, et al., (Plenum Press, 1998), p. 349-371
3. M. Le Tacon, et al., E-print arXiv:1106.2641 (2011).
4. A. A. Vladimirov, D. Ihle, and N. M. Plakida, Phys. Rev. B **80**, 104425 (2009).
5. A. A. Vladimirov, D. Ihle, and N. M. Plakida, Phys. Rev. B **83**, 024411 (2011).
6. H. Mori, Prog. Theor. Phys. **34**, 399 (1965).
7. A. A. Vladimirov, D. Ihle, and N. M. Plakida, Theor. Math. Phys. **145**, 1576 (2005).
8. I. Sega, et al., Phys. Rev. B **68**, 054524, (2003).
9. M. A. Kastner, et al., Rev. Mod. Phys. **40**, 897 (1998).
10. C. Stock, et al., Phys. Rev. B **69**, 014502 (2004).
11. V. Hinkov, et al., Nat. Phys. **3**, 780 (2007).
12. N. M. Plakida, *High-Temperature Cuprate Superconductors* (Springer, Heidelberg, 2010), 570 pp..
13. N. M. Plakida et al., Phys. Rev. B **59**, 11949 (1999).
14. N. M. Plakida, et al., JETP **97**, 331 (2003).
15. T. Cuk, et al., phys. stat. sol. (b) **242**, 11 (2005).
16. E. G. Maksimov, M. L. Kulić, and O. V. Dolgov, Adv. in Cond. Mat. Physics, Article ID 423725 (2010).
17. R. Heid, et al., Phys. Rev. Lett. **100**, 137001 (2008).
18. R. Khasanov, A. Shengelaya, E. Morenzoni, et al., J. Phys.: Condens. Matter **16**, S4439 (2004).
19. Guo-meng Zhao, Phys. Scr. **83** (2011) 038302.
20. A. S. Alexandrov, J. Phys.: Cond. Matter **19**, 125216 (2007).
21. J. Lee, et al., Nature **42**, 546 (2006).
22. J. M. Bok, et al., Phys. Rev. B **81**, 174516 (2010).
23. W. Zhang, et al., E-print arXiv:1103.3629 (2011).